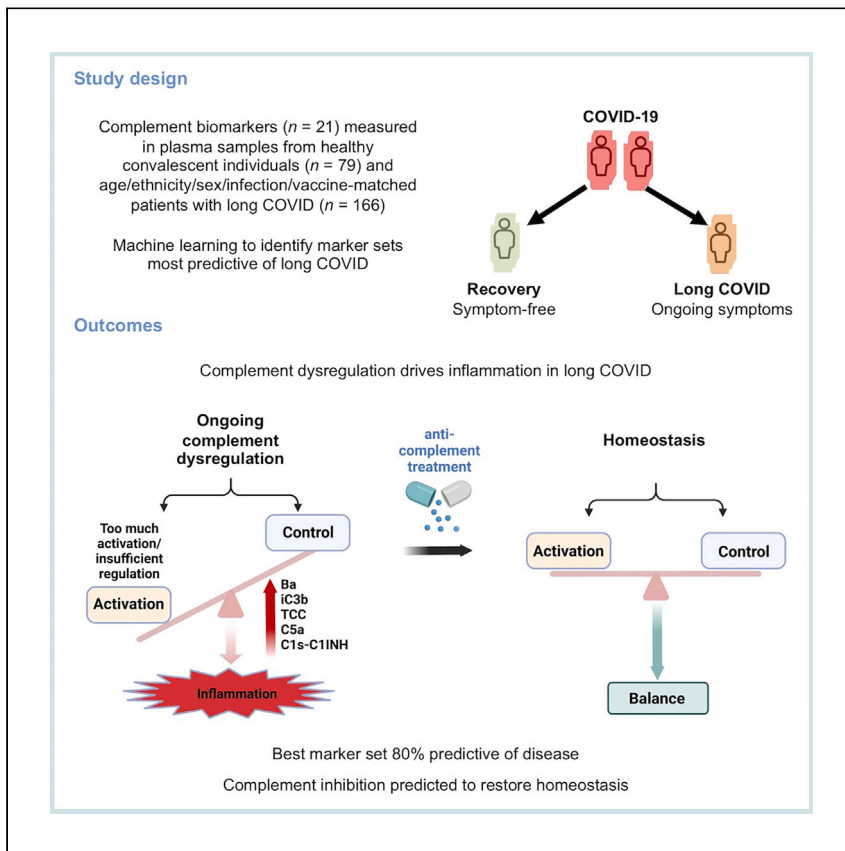


Clinical and Translational Article

Complement dysregulation is a prevalent and therapeutically amenable feature of long COVID



Kirsten Baillie, Helen E. Davies, Samuel B.K. Keat, ..., David A. Price, B. Paul Morgan, Wioleta M. Zelek

morganbp@cardiff.ac.uk

Highlights

Complement dysregulation is a hallmark of long COVID

Complement biomarkers associate with the diagnosis of long COVID

Complement inhibition is a potential therapy for long COVID

Long COVID is a heterogeneous and poorly understood illness triggered by infection with SARS-CoV-2. In this study, Baillie et al. show that complement dysregulation, a known driver of systemic inflammation, is a common and highly indicative feature of long COVID.



Translation to Patients

Clinical and Translational Article

Complement dysregulation is a prevalent and therapeutically amenable feature of long COVID

Kirsten Baillie,^{1,6} Helen E. Davies,^{2,6} Samuel B.K. Keat,^{1,6} Kristin Ladell,¹ Kelly L. Miners,¹ Samantha A. Jones,² Ermioni Mellou,¹ Erik J.M. Toonen,³ David A. Price,^{1,4,5} B. Paul Morgan,^{1,4,5,7,*} and Wioleta M. Zelek^{1,4,5}

SUMMARY

Background: Long COVID encompasses a heterogeneous set of ongoing symptoms that affect many individuals after recovery from infection with SARS-CoV-2. The underlying biological mechanisms nonetheless remain obscure, precluding accurate diagnosis and effective intervention. Complement dysregulation is a hallmark of acute COVID-19 but has not been investigated as a potential determinant of long COVID.

Methods: We quantified a series of complement proteins, including markers of activation and regulation, in plasma samples from healthy convalescent individuals with a confirmed history of infection with SARS-CoV-2 and age/ethnicity/sex/infection/vaccine-matched patients with long COVID.

Findings: Markers of classical (C1s-C1INH complex), alternative (Ba, iC3b), and terminal pathway (C5a, TCC) activation were significantly elevated in patients with long COVID. These markers in combination had a receiver operating characteristic predictive power of 0.794. Other complement proteins and regulators were also quantitatively different between healthy convalescent individuals and patients with long COVID. Generalized linear modeling further revealed that a clinically tractable combination of just four of these markers, namely the activation fragments iC3b, TCC, Ba, and C5a, had a predictive power of 0.785.

Conclusions: These findings suggest that complement biomarkers could facilitate the diagnosis of long COVID and further suggest that currently available inhibitors of complement activation could be used to treat long COVID.

Funding: This work was funded by the National Institute for Health Research (COV-LT2-0041), the PolyBio Research Foundation, and the UK Dementia Research Institute.

INTRODUCTION

The severe acute respiratory syndrome coronavirus 2 (SARS-CoV-2) pandemic left a legacy of chronic illness in a large proportion of survivors of acute coronavirus disease 19 (COVID-19). Encapsulated under the umbrella term “post-acute sequelae of SARS-CoV-2,” the presence of new or ongoing symptoms more than 12 weeks after the acute infection is most commonly known as long COVID.^{1–3} The spectrum of disease is extensive and variable. Common symptoms include cognitive blunting, also called “brain fog,” chest pain, dyspnea, fatigue, and sensory dysregulation, which often have a substantial impact on daily activities and quality of life, akin to myalgic encephalomyelitis/chronic fatigue syndrome.⁴ A recent systematic review concluded

CONTEXT AND SIGNIFICANCE

SARS-CoV-2 has left a global legacy of ill health, commonly known as long COVID. Although the causes of this new disease remain largely unknown, emerging evidence suggests an important role for chronic inflammation. In this study, researchers at Cardiff University show that overactivation of the complement system, a series of proinflammatory proteins circulating throughout the body, frequently associates with the clinical diagnosis of long COVID. The authors speculate that currently licensed inhibitors of complement activation could be repurposed to reduce systemic inflammation and counteract the associated illness in selected patients with long COVID.

that 45% of individuals experience diverse and unresolved symptoms 4 months after infection with SARS-CoV-2, irrespective of initial disease severity.⁵ Chronic disease is also common. For example, a recent national survey (<https://www.ons.gov.uk/peoplepopulationandcommunity/healthandsocialcare/conditionsanddiseases/articles/coronaviruscovid19latestinsights/infections#long-covid>) found that 1.9 million people (2.9% of the population) reported symptoms compatible with long COVID in the UK, with an estimated 41% of affected individuals experiencing ongoing ill health for at least 2 years as of March 2023.

Despite the profound burden of suffering and socioeconomic consequences of long COVID, it remains unclear how chronic illness develops and persists after infection with SARS-CoV-2. Several mechanisms have been proposed to account for the pathogenesis of long COVID, including viral persistence, endothelial dysfunction, coagulation defects, and immune dysregulation.⁶ Persistent inflammation, signposted by elevated blood concentrations of C-reactive protein and proinflammatory cytokines, has also been reported in people with long COVID.^{7,8} The underlying causes of this inflammatory process nonetheless remain obscure. Dysregulation of the complement cascade has been implicated as a driver of inflammation in many diseases, including acute COVID-19.^{9–12} Indeed, the complement system is markedly dysregulated in severe acute COVID-19, and biomarkers spanning all activation pathways predict disease outcome.^{10,13–17} On the basis of these observations, we hypothesized that complement dysregulation could play a key role in the pathogenesis of long COVID.

To evaluate this hypothesis, we conducted an extensive analysis of the complement system in plasma samples obtained from a large cohort of age/ethnicity/sex/infection/vaccine-matched healthy convalescent individuals and non-hospitalized patients with long COVID. Activation products demarcating the classical, alternative, and terminal complement pathways were significantly elevated in patients with long COVID relative to healthy convalescent individuals with no persistent symptoms after recovery from infection with SARS-CoV-2. Plasma concentrations of some complement components and regulators also differed significantly between healthy convalescent individuals and patients with long COVID. Moreover, various combinations of these analytes, including minimal panels with clinical applicability, were highly predictive of disease. These findings implicate complement dysregulation as a driver of inflammation and provide a novel set of biomarkers that could guide the diagnosis and treatment of long COVID.

RESULTS

Cohort description and study overview

Plasma samples were collected from healthy convalescent individuals (controls, $n = 79$) and patients with long COVID (cases, $n = 166$). All participants had a clearly defined episode of acute COVID-19 confirmed via direct molecular evidence of infection with SARS-CoV-2. Reinfections were detected uncommonly (cases, $n = 12$; controls, $n = 6$). Groups were matched for age (cases, median = 47 years; controls, median = 45 years), ethnicity (cases, White = 88.0%; controls, White = 84.8%), sex (cases, female = 76.5%; controls, female = 78.5%), infection wave (cases, 54.8% infected more than 2 years before sample acquisition; controls, 46.8% infected more than 2 years before sample acquisition), and vaccination status (cases, median number of vaccinations before infection = 2; controls, median number of vaccinations before infection = 3), a parameter known to mitigate the risk of long COVID.¹⁸ At enrollment, all medical evaluations, including chest radiography,

¹Division of Infection and Immunity, Cardiff University School of Medicine, University Hospital of Wales, Heath Park, Cardiff CF14 4XN, UK

²Department of Respiratory Medicine, University Hospital of Wales, Llandough, Penarth CF64 2XX, UK

³R&D Department, Hycult Biotechnology, Frontstraat 2A, 5405 PB Uden, the Netherlands

⁴Systems Immunity Research Institute, Cardiff University School of Medicine, University Hospital of Wales, Heath Park, Cardiff CF14 4XN, UK

⁵Senior author

⁶These authors contributed equally

⁷Lead contact

*Correspondence: morganbp@cardiff.ac.uk
<https://doi.org/10.1016/j.medj.2024.01.011>

electrocardiography, lung function tests (spirometry with gas transfer as indicated and measurement of exhaled nitric oxide), and standard blood tests (autoantibody screens; bone, liver, and kidney function; coagulation screens; full blood count; and markers of nutrition) were normal in patients with long COVID. Of note, obesity (BMI >30) was significantly more common in cases versus controls (48.8% versus 34.6%, respectively, $p = 0.042$), and although employment status was comparable between groups pre-acute COVID-19, only 43.6% of cases remained in full-time work post-acute COVID-19 compared with 89.1% pre-acute COVID-19 ($p < 0.00001$). Cohort demographics, symptomatology, and other key features are summarized in [Table 1](#).

Complement activation products are elevated in patients with long COVID

The role of complement dysregulation as a potential determinant of long COVID symptomatology has not been investigated previously. To address this knowledge gap, we quantified six markers of complement activation, including classical, lectin, alternative, and terminal pathway products, comparing plasma concentrations in healthy convalescent individuals (controls, $n = 79$) and patients with long COVID (cases, $n = 166$). The C1s-C1 inhibitor (C1INH) complex, a product of classical pathway activation, was significantly elevated in cases versus controls (1.25 versus 1.09 $\mu\text{g/mL}$, respectively, $p = 0.0089$), whereas no such differences were observed for the mannose-associated serine protease 1 (MASP1)-C1INH complex, generated during lectin pathway activation (65.0 versus 56.8 ng/mL , respectively, $p = 0.15$) ([Figures 1A and 1B](#)). The fragments iC3b and Ba, which indicate alternative pathway activation, were also significantly elevated in cases versus controls (iC3b, 20.7 versus 14.4 $\mu\text{g/mL}$, respectively, $p < 0.0001$; Ba, 0.39 versus 0.22 $\mu\text{g/mL}$, respectively, $p < 0.001$) ([Figures 1C and 1D](#)). In addition, C5a and the terminal complement complex (TCC), which demarcate terminal pathway activation, were both significantly elevated in cases versus controls, with the latter demonstrating a substantial increase (C5a, 7.45 versus 5.09 ng/mL , respectively, $p < 0.02$; TCC, 5.56 versus 3.55 $\mu\text{g/mL}$, respectively, $p < 0.0001$) ([Figures 1E and 1F](#)). Assay details are provided in [Table S1](#), and the results are summarized in [Table 2](#).

Complement components and regulators are altered in patients with long COVID

In parallel, we quantified a series of complement components and regulators in the same samples, again comparing plasma concentrations in healthy convalescent individuals (controls, $n = 79$) and patients with long COVID (cases, $n = 166$). C1q, the trigger for classical pathway activation, was significantly lower in cases versus controls (109.2 versus 130 $\mu\text{g/mL}$, respectively, $p < 0.05$), likely reflecting consumption ([Figure 2A](#)). In contrast, C3, C5, and C9 were all significantly elevated in cases versus controls (C3, 0.89 versus 0.83 $\mu\text{g/mL}$, respectively, $p < 0.01$; C5, 198.4 versus 174.5 $\mu\text{g/mL}$, respectively, $p < 0.005$; C9, 92.5 versus 83.2 $\mu\text{g/mL}$, respectively, $p < 0.01$) ([Figures 2D–2F](#)). All three of these proteins are positive acute phase reactants, likely explaining the increased concentrations in patients with long COVID. Levels of C4 and factor B (FB) were also higher in cases versus controls, albeit not significantly ([Figures 2B and 2C](#)). Assay details are provided in [Table S1](#), and the results are summarized in [Table 2](#).

Most of the complement regulators selected for measurement were also significantly elevated in cases versus controls, including C1INH, the key regulator of classical and lectin pathway activation (113.7 versus 100.9 $\mu\text{g/mL}$, respectively, $p < 0.001$) ([Figure 3A](#)); FD, FH, and properdin, which are involved in the regulation of alternative pathway activation (FD, 0.92 versus 0.70 $\mu\text{g/mL}$, respectively, $p < 0.0001$; FH, 263.4 versus 232.3 $\mu\text{g/mL}$, respectively, $p < 0.01$; properdin, 3.88 versus

Table 1. Demographics, symptomatology, and other key features of healthy convalescent individuals and patients with long COVID

Characteristic	Controls (n = 79)	Long COVID (n = 166)
Age (years), median (range)	45 (21–82)	47 (20–83)
Female (%)	62 (78.5)	127 (76.5)
Ethnicity/race (%)		
White	67 (84.8)	146 (88.0)
Black	0 (0.0)	3 (1.8)
Asian	8 (10.2)	8 (4.8)
Mixed ethnicity	2 (2.5)	2 (1.2)
Other	2 (2.5)	7 (4.2)
Body mass index >30 kg/m ² (%)	26/75 (34.6)	79/162 (48.8)
Coexisting conditions (%)		
Yes	14 (17.7)	55 (33.1)
No	65 (82.3)	111 (66.9)
Employment status (%)		
Pre-COVID-19		
Employed	53 (91.4)	139 (89.1)
Employed, altered duties	0 (0.0)	0 (0.0)
Employed, sick leave	0 (0.0)	0 (0.0)
Unemployed	0 (0.0)	4 (2.6)
Retired	2 (3.4)	11 (7.0)
Student	3 (5.2)	2 (1.3)
Post-COVID-19		
Employed	54 (93.2)	68 (43.6)
Employed, altered duties	0 (0.0)	28 (17.9)
Employed, sick leave	0 (0.0)	33 (21.2)
Unemployed	0 (0.0)	11 (7.1)
Retired	2 (3.4)	13 (8.3)
Student	2 (3.4)	3 (1.9)
Date of infection with SARS-CoV-2 (%)		
March 2020 to August 2020	14 (17.7)	34 (20.5)
September 2020 to June 2021	23 (29.1)	57 (34.3)
July 2021 to October 2022	42 (53.2)	75 (45.2)
COVID-19 vaccination status, median (IQR)		
No. of vaccinations before infection	3 (0–3)	2 (0–2)
Total number of vaccinations	3 (3–3)	3 (3–3)
Symptoms ^a		
Breathlessness	0 (0–0)	4 (2–6)
Fatigue	0 (0–2)	6 (4–8)
Musculoskeletal	0 (0–0)	3 (0–6)
Neuropsychiatric	0 (0–0)	3 (1–5)
Pain	0 (0–0)	4 (2–6)
Ability to maintain self-care	0 (0–0)	0 (0–3)
Ability to maintain daily tasks	0 (0–0)	6 (3–8)
Overall general health ^b	0 (0 to –1)	–4 (–2 to –6)

^aDifference in numeric rating scale score (0 = no symptom, 10 = worst possible symptom) before versus after COVID-19 (median ± IQR).

^bDifference in numeric rating scale score (0 = worst possible, 10 = best possible) before versus after COVID-19 (median ± IQR).

2.99 µg/mL, respectively, $p < 0.0001$) (Figures 3B–3D); and clusterin, a regulator of the terminal pathway (145.6 versus 130.6 µg/mL, respectively, $p < 0.05$) (Figure 3E). Plasma levels of the key alternative pathway regulator FI, the soluble form of complement receptor 1 (sCR1), and the FH-related (FHR) proteins (FHR4 and FHR125) were not significantly different between healthy convalescent individuals and patients

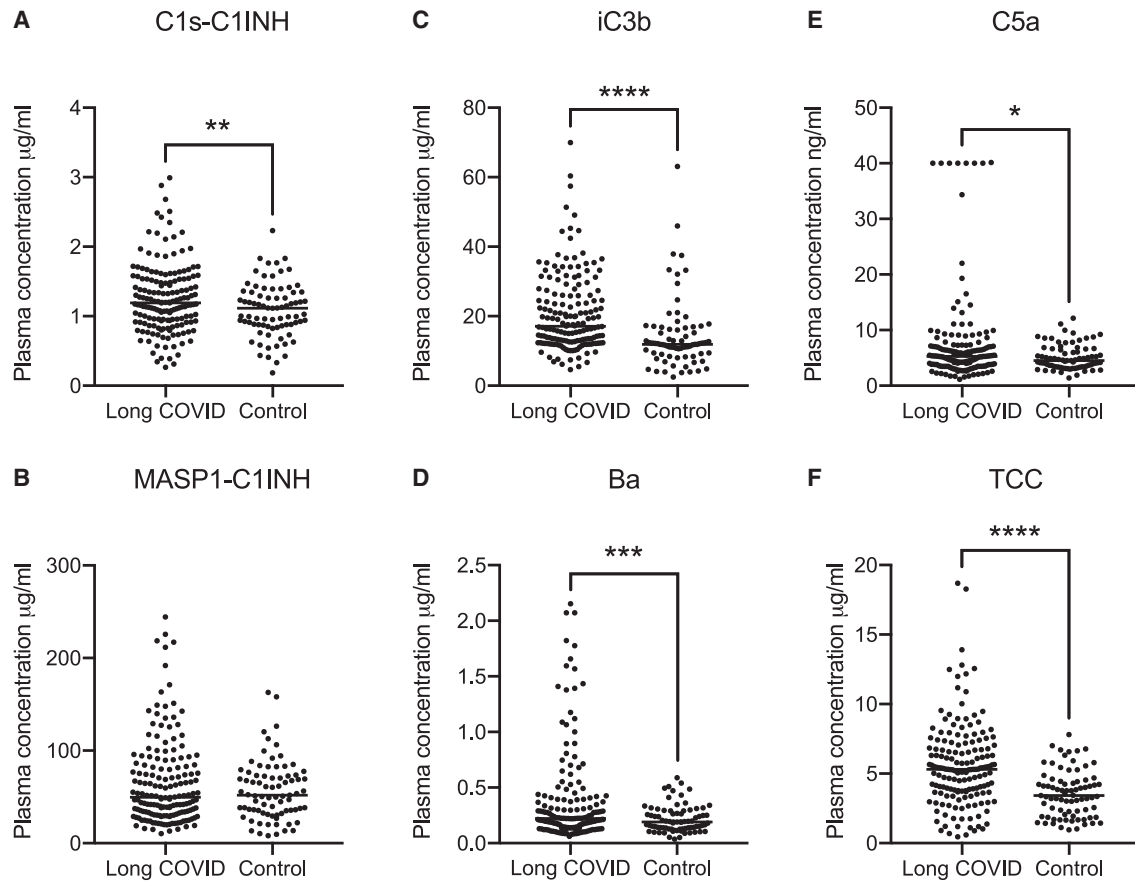


Figure 1. Plasma concentrations of complement activation products in healthy convalescent individuals and patients with long COVID

Dot plots showing plasma concentrations of C1s-C1INH (A), MASP1-C1INH (B), iC3b (C), Ba (D), C5a (E), and TCC (F) in healthy convalescent individuals (n = 79) and patients with long COVID (n = 166). Horizontal bars represent mean values. *p < 0.05, **p < 0.01, ***p < 0.001, and ****p < 0.0001 (unpaired t test).

with long COVID (Figures 3F and S1A–S1C). Of note, there were also no differences in plasma hemolytic activity or anti-SARS-CoV-2 spike protein receptor-binding domain (RBD) antibody titers between healthy convalescent individuals and patients with long COVID (Figures S1D and S1E). Assay details are provided in Table S1, and the results are summarized in Table 2.

Complement biomarker sets identify patients with long COVID

Plasma concentration distributions for each complement protein measured in this study (n = 21) are shown for cases and controls as density plots in Figure 4A and as scatterplots versus age in Figure 4B. The associated statistics are shown in Table S2. Pearson correlograms are shown in Figure 5. These latter comparisons revealed strong positive correlations between various pairs of analytes (Figures 5A and 5B), most notably among the complement activation products (Ba, iC3b, and TCC) (Figures 5E and 5H) but also among the complement components (C3, C4, C5, and C9) (Figures 5D and 5G) and regulators (FH, FD, and FI) (Figures 5C and 5F). In receiver operating characteristic (ROC) analyses using multiple generalized linear models (GLMs), 9/21 complement proteins measured in our panels showed good predictive power (area under the curve [AUC] > 0.6), including three activation products (ranked iC3b, TCC, and Ba) and six other markers (ranked C1INH, FD, C3,

Table 2. Complement biomarker concentrations in healthy convalescent individuals and patients with long COVID

	Units	Controls	Cases	p
Activation products				
C1s-C1INH	μg/mL	1.088	1.255	0.0089 ^a
MASP1-C1INH	ng/mL	56.75	65.03	0.154
Ba	μg/mL	0.2172	0.3871	0.0007 ^a
iC3b	μg/mL	14.36	20.72	<0.0001 ^a
C5a	ng/mL	5.090	7.454	0.0135 ^a
TCC	μg/mL	3.551	5.559	<0.0001 ^a
Components				
C1q	μg/mL	130	109.2	0.0312 ^a
C4	μg/mL	511.8	477.8	0.1341
C3	μg/mL	830.2	893.3	0.0102 ^a
FB	μg/mL	279.7	268.7	0.5314
C5	μg/mL	174.5	198.4	0.0037 ^a
C9	μg/mL	83.2	92.52	0.0103 ^a
Regulators				
C1INH	μg/mL	100.9	113.7	0.0011 ^a
FH	μg/mL	232.3	263.4	0.079
FHR125	μg/mL	101.7	113.9	0.2866
FHR4	μg/mL	3.879	3.883	0.9824
sCR1	ng/mL	6.759	6.436	0.2141
Properdin	μg/mL	2.994	3.878	<0.0001 ^a
FD	μg/mL	0.6977	0.922	<0.0001 ^a
FI	μg/mL	54.17	56.53	0.2468
Clusterin	μg/mL	130.6	145.6	0.043 ^a

Mean values are shown. Significance was determined using an unpaired t test. C1INH, C1 inhibitor; MASP1, mannose-associated serine protease 1; TCC, terminal complement complex; FB, factor B; FH, factor H; FHR125, FH-related proteins 1, 2, and 5; FHR4, FH-related protein 4; sCR1, soluble complement receptor 1; FD, factor D; FI, factor I.

^aSignificant difference.

properdin, C9, and FH) (Figures 6A and 6B). The most predictive single marker was C1INH, with an AUC of 0.746 (Figure 6B).

The impact of combining the most predictive biomarkers was then tested in ROC analyses via step Akaike information criterion (stepAIC) model selection. The best model contained TCC, Ba, C1q, C4, C5, C1INH, FD, and properdin, with an overall AUC of 0.825 and an AIC of 141.85 (Figure 6C). Sequential regressive steps from the best stepAIC method did not significantly improve either the AUCs or the AICs. In a second analysis focused on activation markers, the combination of iC3b, TCC, Ba, and C5a increased the AUC (0.729 to 0.785) relative to iC3b alone (Figure 6D). Inclusion of the other two activation markers, C1s-C1INH and MASP1-C1INH, had no significant impact on the AUC (Figure 6D). Forest plots are shown in Figure S2. Details of all ROC-AUC analyses showing predictive statistics for adjusted and unadjusted GLMs, stepAIC-informed GLMs, and sequential activation GLMs, as well as main confounder (age, sex, and BMI) tests of the GLMs, are provided in Tables S3–S7.

We then conducted a principal component analysis (PCA) (Figure S3A). Visualization of individual sample contributions to the first two principal components (PCs) revealed considerable overlap between healthy convalescent individuals and patients with long COVID (Figure S3B). The first two PCs explained 35% of the total variance (20.2% for PC1 and 14.8% for PC2) (Figure S3C). C3 made the greatest contribution

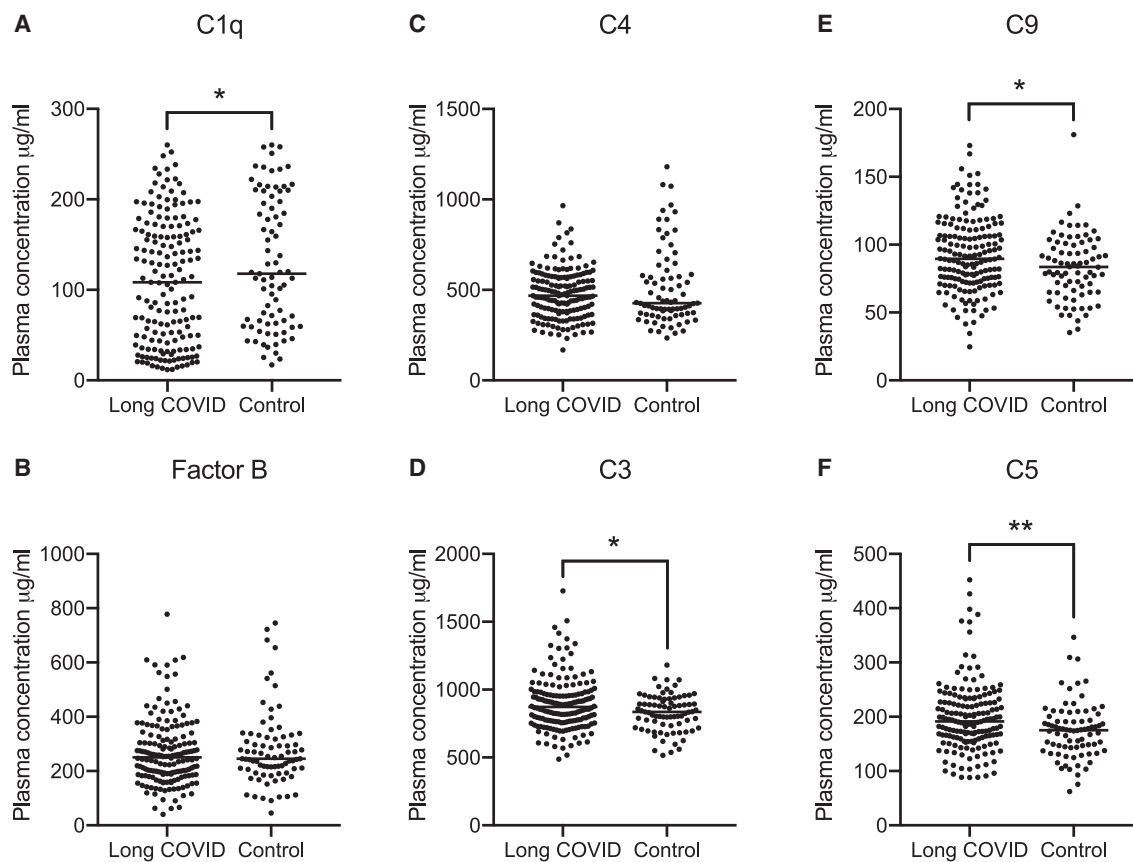


Figure 2. Plasma concentrations of complement components in healthy convalescent individuals and patients with long COVID

Dot plots showing plasma concentrations of C1q (A), factor B (B), C4 (C), C3 (D), C9 (E), and C5 (F) in healthy convalescent individuals ($n = 78-79$) and patients with long COVID ($n = 166$). Horizontal bars represent mean values. * $p < 0.05$ and ** $p < 0.01$ (unpaired t test).

to PC1 (17.27%), followed by C9 (12.7%) and C5 (11.21%) (Figure S3D), whereas Ba made the greatest contribution to PC2 (9.74%), followed by C1INH (9.05%) and FHR125 (9.03%) (Figure S3E).

Collectively, these data and the associated analyses, especially the GLMs, demonstrate that complement dysregulation is a consistent and predictive feature of long COVID.

DISCUSSION

Complement dysregulation is a common feature of diverse acute and chronic inflammatory diseases and a major driver of inflammation. There is abundant evidence from biomarker studies to indicate that complement dysregulation involving all activation pathways is ubiquitous during acute infection with SARS-CoV-2, especially in individuals with severe COVID-19.¹⁰⁻¹⁷ Moreover, admission levels of several complement biomarkers, including the activation fragment Ba, predict outcome in hospitalized patients with acute COVID-19.¹⁰ Progressive changes in the concentrations of some complement biomarkers have also been reported in the context of severe disease.^{10,14-17,19} In mechanistic terms, complement activation under these circumstances has been variously attributed to direct virus-mediated triggering of the classical, lectin, and/or alternative pathways, activation of the classical pathway via

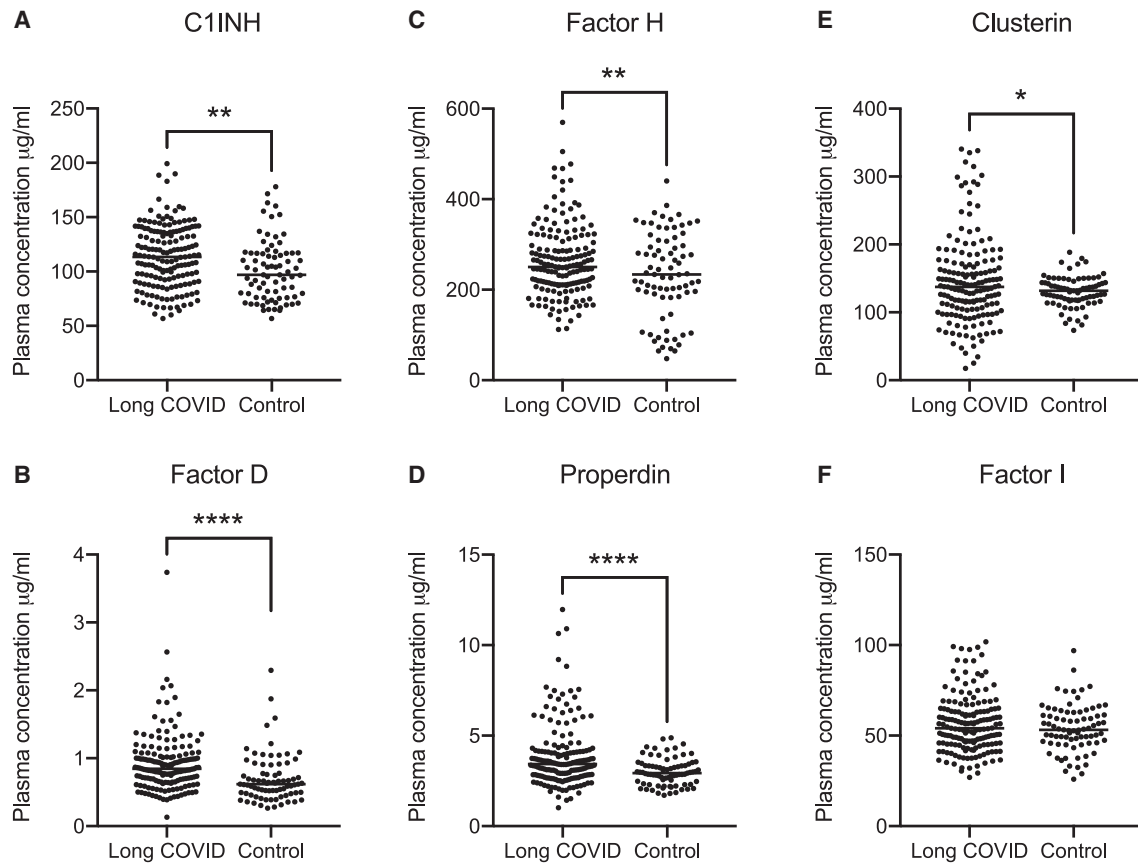


Figure 3. Plasma concentrations of complement regulators in healthy convalescent individuals and patients with long COVID

Dot plots showing plasma concentrations of C1INH (A), factor D (B), factor H (C), properdin (D), clusterin (E), and factor I (F) in healthy convalescent individuals (n = 78–79) and patients with long COVID (n = 166). Horizontal bars represent mean values. *p < 0.05, **p < 0.01, and ****p < 0.0001 (unpaired t test).

antiviral antibodies, and/or indirect activation via contact with infected cells and/or damaged tissue.^{20–24}

These observations have been used to rationalize interventions with complement blocking drugs to mitigate the hyperinflammatory state that characterizes severe COVID-19. Early pilot studies reported positive effects using repurposed existing drugs to inhibit complement activation or the terminal pathway.^{25–30} However, the numerous clinical trials of agents targeting C5, C5a/C5aR, C3, FD, or C1 that followed have been disappointing to date, potentially reflecting a failure to screen for complement dysregulation prior to inclusion, a focus on the most severe cases, and/or treatment late in the disease course.³¹

Persistent inflammation has been implicated as a key component of long COVID. In particular, elevated levels of inflammatory cytokines and the inflammatory markers C-reactive protein and serum amyloid A were detected in a study of symptomatic patients 6–9 months after acute infection with SARS-CoV-2,⁷ and a systematic review compiling data from 22 studies confirmed an association between elevated plasma concentrations of interleukin-6 and long COVID.⁸ High titers of various autoantibodies, notably those associated with myopathies, vasculitides, and other related conditions, have also been reported in long COVID.³² In another study,

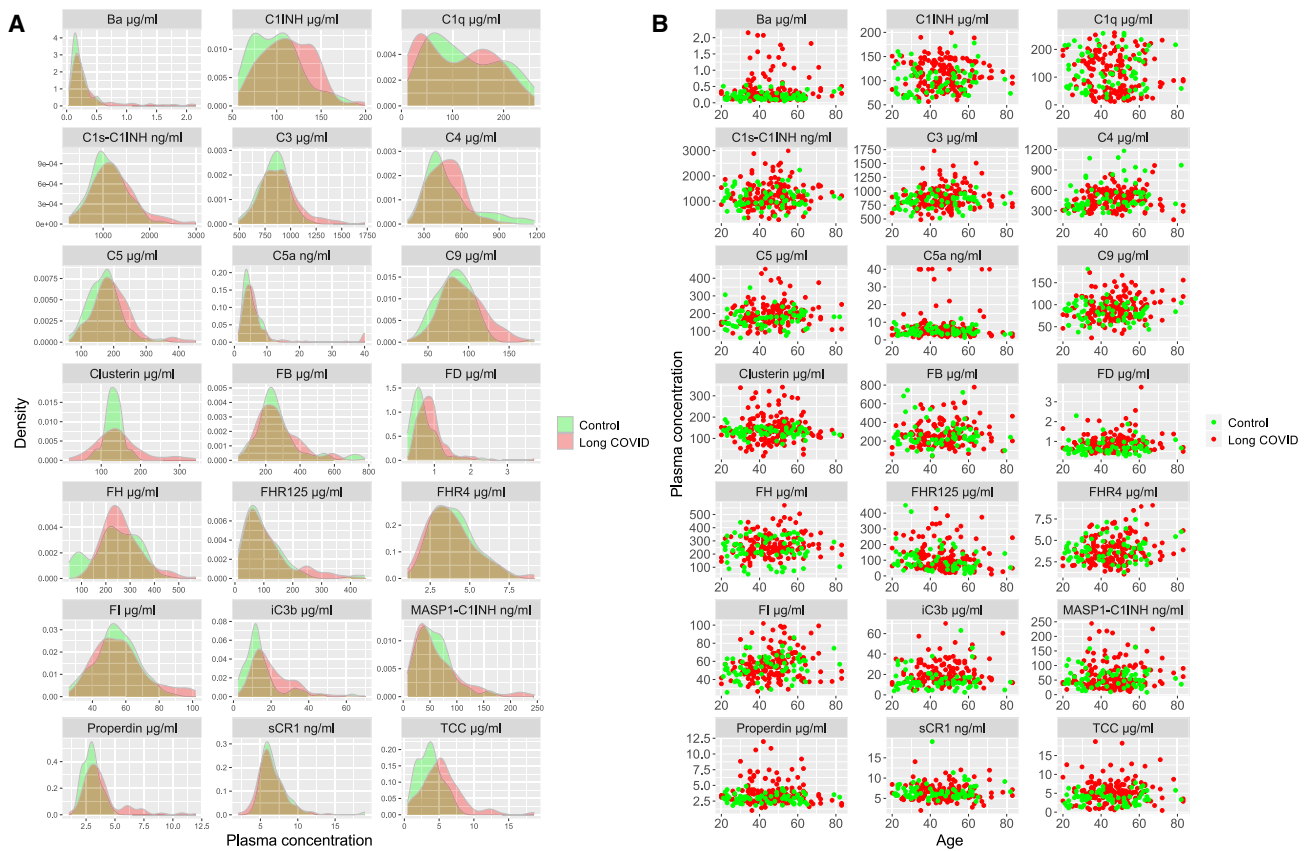


Figure 4. Plasma concentration distributions for complement proteins in healthy convalescent individuals and patients with long COVID
(A) Density plots showing the plasma concentration distribution for each complement analyte ($n = 21$) in healthy convalescent individuals (green, $n = 78-79$) and patients with long COVID (red, $n = 166$).
(B) Scatterplots showing the plasma concentration distribution for each complement analyte ($n = 21$) versus age at inclusion in healthy convalescent individuals (green, $n = 78-79$) and patients with long COVID (red, $n = 166$).

autoantibodies against inflammatory chemokines were found to be common in the convalescent phase and correlated with better outcomes and a lower risk of developing long COVID.³³ Innate immune cell activation has also been identified as a driver of lung fibrosis and inflammation in a humanized mouse model of long COVID.³⁴

All of these reports point to immune dysregulation with attendant inflammation as critical determinants of long COVID, but none identify an obvious inflammatory trigger or target for therapy.³ In this study, we set out to test whether persistent complement dysregulation contributed to the pathophysiology of long COVID. We found that markers of complement activation spanning the classical (C1s-C1INH), alternative (iC3b, Ba), and terminal pathways (C5a, TCC), but not the lectin pathway (MASP1-C1INH), were all significantly elevated in patients with long COVID compared with healthy convalescent individuals infected during the same wave of SARS-CoV-2. In a previous study, we found that Ba, iC3b, and TCC stood out as markers of disease course and outcome in patients with acute COVID-19.¹⁰ Moreover, plasma concentrations of iC3b and TCC remained elevated in convalescent samples up to a median of 21 days after discharge, indicating persistent complement dysregulation.¹⁰ It is particularly notable here that C5a, a leukocyte activator

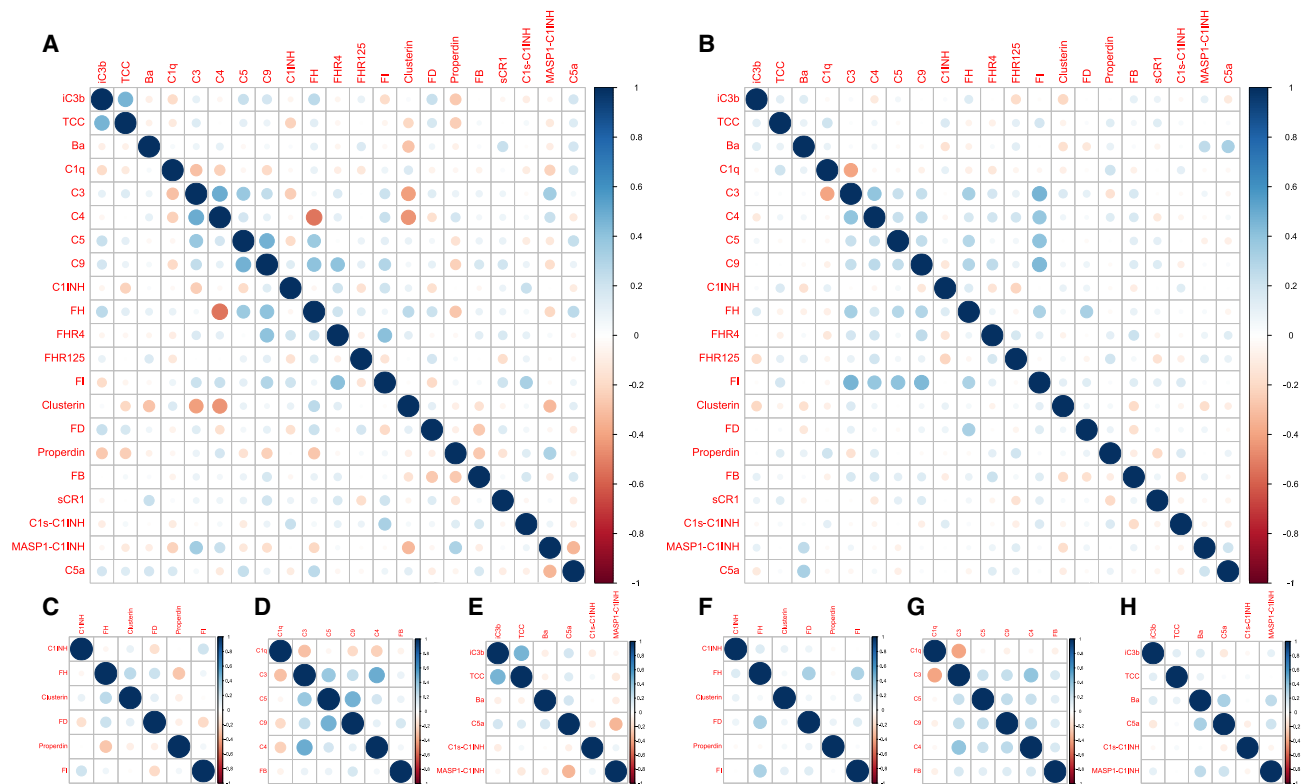


Figure 5. Complement analyte correlograms for healthy convalescent individuals and patients with long COVID

Correlograms are shown for all complement analytes measured in plasma samples from healthy convalescent individuals (A) and patients with long COVID (B) and separately by group for complement regulatory proteins (C and F, respectively), complement components (D and G, respectively), and complement activation products (E and H, respectively). The size of each circle indicates the strength of the correlation, and colors show the intensity of direct (dark blue) or inverse (dark red) correlations, each measured using the Pearson correlation coefficient (r).

and chemoattractant, and TCC, a proxy for membrane attack complex (MAC) formation, are both potent triggers of inflammation and collaborate across diverse cell types to activate the inflammasome pathway.^{35,36}

In further assays, we found that plasma concentrations of many complement components were also relatively elevated in patients with long COVID. These observations could be explained by the fact that C3, C4, C5, and C9 are all positive acute phase reactants, such that measured plasma levels reflect the net effect of consumption caused by complement activation and increased synthesis driven by inflammation.³⁷ In contrast, plasma concentrations of C1q, which is not an acute phase reactant, were significantly lower in cases versus controls, likely reflecting uncompensated consumption. Moreover, we found that plasma concentrations of several complement regulators, namely C1INH, FD, properdin, FH, and clusterin, were relatively elevated in patients with long COVID. Elevated levels of C1INH would be expected to limit activation of the classical and lectin pathways, whereas FD, properdin, and FH all regulate the alternative pathway. Specifically, FD mediates the enzymatic cleavage of FB, which is required to form the alternative pathway convertase C3bBb, and properdin stabilizes C3bBb, such that elevated levels of these regulators would be expected to increase activity in the alternative pathway. In contrast, FH is a negative regulator, catalyzing the inactivation of C3bBb. Activation of the alternative pathway nonetheless dominated in patients with long COVID, as

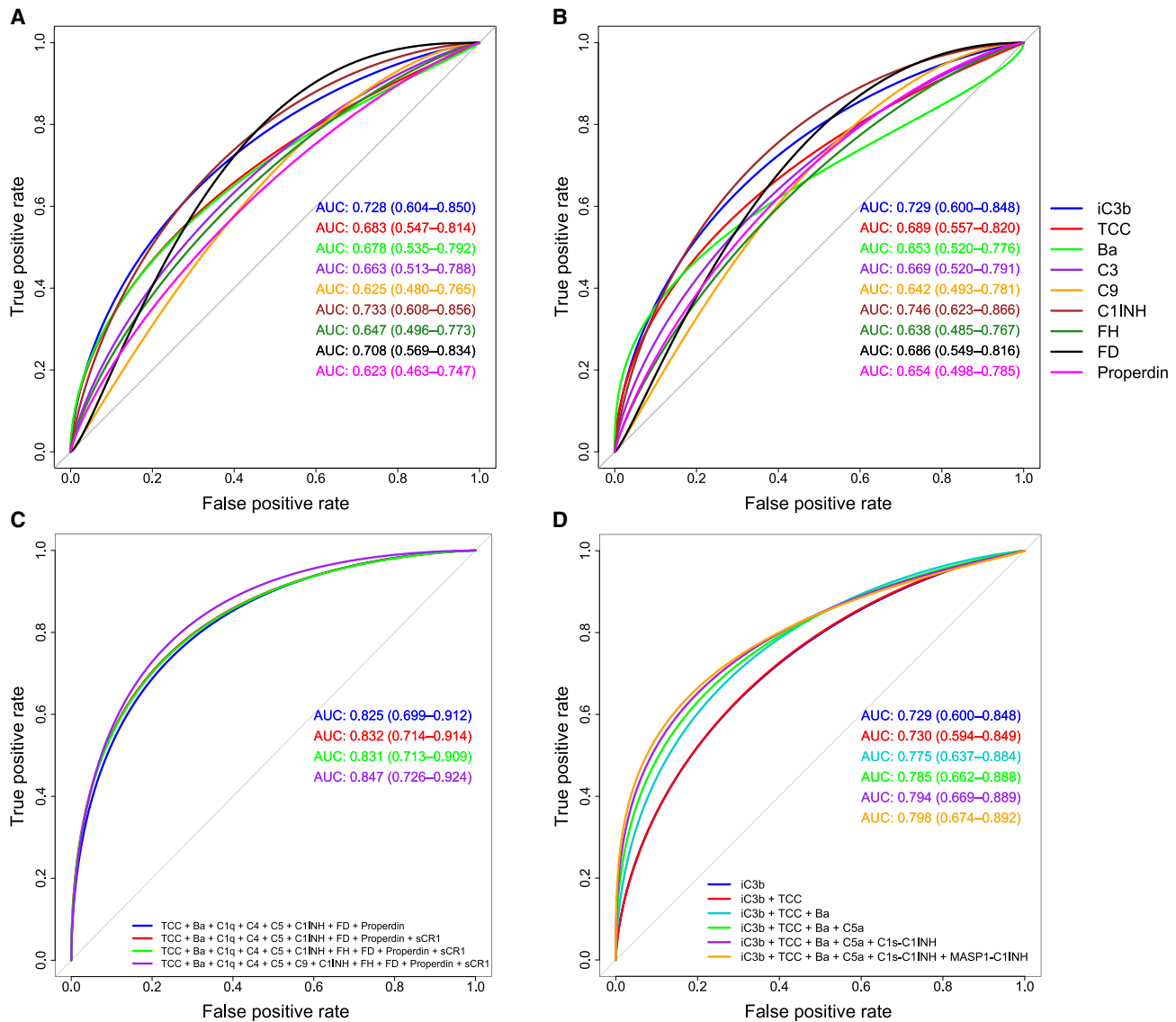


Figure 6. Receiver operator characteristic curves for generalized linear models (GLMs) using complement protein concentrations in plasma to predict long COVID

Receiver operator curves were generated using multiple GLMs for each complement protein. AUC statistics are shown for individual (A and B) or combined analytes (C and D) with 95% confidence intervals (generated from 2,000 bootstrap replicates) in parentheses for each GLM. Proteins were unadjusted (A) or adjusted for age, sex, and BMI (B–D). Linear predictors were selected according to the results of stepAIC models of adjusted protein concentrations (C). The best model was plotted first based on the highest AIC relative to model complexity (TCC + Ba + C1q + C4 + C5 + C1INH + FD + properdin), and then three regressive steps from the stepAIC results were plotted sequentially. Sequential combinations are shown for each of the top ranked AUC statistics from complement activator GLMs (D), starting with the highest ranked AUC (iC3b).

highlighted by the elevated plasma concentrations of Ba and iC3b. Clusterin is a multifunctional plasma lipoprotein that inhibits assembly of the MAC. It is notable here that plasma levels of clusterin were previously found to be reduced in severe acute COVID-19.¹⁰

Data analyses revealed that 9/21 complement analytes measured in our study were predictive of long COVID (AUC > 0.6). The most predictive single biomarker was C1INH, with an AUC of 0.746, and optimal prediction was enabled by a

stepAIC-informed combination of biomarkers incorporating Ba, C1q, C4, C5, C1INH, FD, properdin, and TCC. A more clinically tractable combination of just four activation markers, namely Ba, iC3b, C5a, and TCC, yielded an AUC of 0.785. These biomarker sets focus attention on dysregulation of the alternative pathway amplification loop with activation of the downstream terminal pathway, reminiscent of our findings in acute COVID-19.¹⁰

It remains unclear precisely how complement dysregulation is sustained in patients with long COVID. However, there is now a wealth of evidence to indicate that SARS-CoV-2 can persist in tissue reservoirs long after resolution of the acute infection,³⁸ providing a biologically feasible mechanistic trigger for the inflammatory processes that characterize long COVID. Moreover, SARS-CoV-2 activates the complement system both directly and indirectly, especially via the amplification loop, to drive endothelial damage and inflammation in acute COVID-19.^{39,40} Ongoing viral replication likely does the same in the context of long COVID.

There are no specific therapies for long COVID. Current treatment approaches focus on symptom relief and multidisciplinary rehabilitation.³ A handful of clinical trials are in progress using drugs that target cardiac damage (ivabradine), fibrotic lung injury (pirfenidone, inhaled interferon-1), and inflammation (leronlimab) induced by acute infection with SAR-CoV-2.⁴¹ However, the patients in our cohort exhibited no concomitant symptom-driving pathology, and allied tests for underlying organ dysfunction, as listed above, universally fell within the normal range. Accordingly, our data suggest that complement dysregulation and the associated inflammatory response are potentially viable targets for therapeutic interventions designed to ameliorate symptoms and break the pathogenic cycle of disease, irrespective of the fact that such approaches have proven largely ineffective in the fundamentally different setting of acute COVID-19.³¹ There are now several complement inhibitors in clinical use that could be repurposed to treat long COVID. Our findings suggest that the preferred target is the alternative pathway, which can be suppressed by drugs such as pegcetacoplan (targeting C3), iptacopan (targeting FB), and vemircofan (targeting FD).⁴² It is important to emphasize here that a lack of efficacy in the setting of acute disease does not necessarily invalidate the use of such agents in the setting of chronic disease. Moreover, the availability of reliable complement biomarkers identified in the present study would allow rigorous patient selection and provide objective measures to monitor the impact of any such intervention, potentially informing mechanistic links with symptomatology. On this basis, we propose that pilot trials are now warranted to test the utility of such drugs under close clinical supervision, even for a relatively short period of time, with the aim of disrupting the proinflammatory cycle and restoring a normal pattern of homeostasis in patients with long COVID.

Limitations of the study

Our analysis was cross-sectional in nature, precluding retrospective associations with complement activation and clinical severity at the time of infection, and our study population was predominantly White. Infectious events were also limited to the three major waves of SARS-CoV-2 that circulated previously in the UK. Moreover, the selection of biological confounders as adjustment variables was restricted to age, sex, and BMI, which did not necessarily account for all of the observed variance. Other possible confounders, including the number of reinfections and time since the index infection, were excluded as adjustment variables if the impact was negligible. In addition, statistical power was

Med

Clinical and Translational Article

potentially limited by sample size, given the lack of significance for several complement proteins analyzed in the GLMs. Sample size also precluded meaningful segregation based on dominant symptoms, symptom clusters, or functional disability. It is further notable that our study was not designed to identify the precise triggers of complement activation in long COVID.

STAR★METHODS

Detailed methods are provided in the online version of this paper and include the following:

- KEY RESOURCES TABLE
- RESOURCE AVAILABILITY
 - Lead contact
 - Materials availability
 - Data and code availability
- EXPERIMENTAL MODEL AND STUDY PARTICIPANT DETAILS
 - Donors
 - Ethics
 - Samples
- METHOD DETAILS
 - Immunoassays
 - Anti-RBD IgG assay
 - Hemolytic assay
- QUANTIFICATION AND STATISTICAL ANALYSIS
 - General statistics
 - Receiver operating characteristic analysis
 - Principal component analysis
 - Data visualization

SUPPLEMENTAL INFORMATION

Supplemental information can be found online at <https://doi.org/10.1016/j.medj.2024.01.011>.

ACKNOWLEDGMENTS

We thank all participants for their enthusiastic contributions to this study. This work was funded by the National Institute for Health Research (COV-LT2-0041), the Poly-Bio Research Foundation, and the UK Dementia Research Institute. Additional support was provided via an Alzheimer's Research UK Race Against Dementia Fellowship Award (W.M.Z.). We also thank Lisa Hurler, Erika Kajdácsi, László Cervenak, and Zoltán Prohászka (Department of Medicine and Haematology, Semmelweis University, Budapest, Hungary) for developing the C1s/C1-INH and MASP-1/C1-INH complex ELISAs, which were kindly donated by Loek Willems (Hycult Biotech, Eindhoven, the Netherlands).

AUTHOR CONTRIBUTIONS

K.B., H.E.D., K.L., K.L.M., S.A.J., E.M., E.J.M.T., and W.M.Z. performed experiments and/or provided reagents/resources; S.B.K.K. analyzed data; and H.E.D., D.A.P., B.P.M., and W.M.Z. conceived the project, led the study, supervised the work, and wrote the paper. S.B.K.K., B.P.M., and W.M.Z. had unrestricted access to all data reported in this study. All authors accepted responsibility for the work, approved the final draft of the manuscript, and concurred with the decision to submit for publication.

DECLARATION OF INTERESTS

The authors declare no competing interests.

Received: July 21, 2023

Revised: November 9, 2023

Accepted: January 22, 2024

Published: February 14, 2024

REFERENCES

1. Stoian, M., Procopiescu, B., Şeitan, S., and Scarlat, G. (2023). Post-COVID-19 syndrome: insights into a novel post-infectious systemic disorder. *J. Med. Life* 16, 195–202.
2. Sherif, Z.A., Gomez, C.R., Connors, T.J., Henrich, T.J., and Reeves, W.B.; RECOVER Mechanistic Pathway Task Force (2023). Pathogenic mechanisms of post-acute sequelae of SARS-CoV-2 infection (PASC). *Elife* 12, e86002.
3. Schmidt, C. (2021). COVID-19 long haulers. *Nat. Biotechnol.* 39, 908–913.
4. Komaroff, A.L., and Lipkin, W.I. (2023). ME/CFS and long COVID share similar symptoms and biological abnormalities: road map to the literature. *Front. Med.* 10, 1187163.
5. O'Mahoney, L.L., Routen, A., Gillies, C., Ekezie, W., Welford, A., Zhang, A., Karamchandani, U., Simms-Williams, N., Cassambai, S., Ardavani, A., et al. (2023). The prevalence and long-term health effects of Long Covid among hospitalised and non-hospitalised populations: a systematic review and meta-analysis. *eClinicalMedicine* 55, 101762.
6. Castanares-Zapatero, D., Chalou, P., Kohn, L., Dauvin, M., Detollenaere, J., Maertens de Noordhout, C., Primus-de Jong, C., Cleemput, I., and Van den Heede, K. (2022). Pathophysiology and mechanism of long COVID: a comprehensive review. *Ann. Med.* 54, 1473–1487.
7. Ahearn-Ford, S., Lunjani, N., McSharry, B., MacSharry, J., Fanning, L., Murphy, G., Everard, C., Barry, A., McGreal, A., Al Lawati, S.M., et al. (2021). Long-term disruption of cytokine signalling networks is evident in patients who required hospitalization for SARS-CoV-2 infection. *Allergy* 76, 2910–2913.
8. Yin, J.X., Agbana, Y.L., Sun, Z.S., Fei, S.W., Zhao, H.Q., Zhou, X.N., Chen, J.H., and Kassegne, K. (2023). Increased interleukin-6 is associated with long COVID-19: a systematic review and meta-analysis. *Infect. Dis. Poverty* 12, 43.
9. Morgan, B.P., and Harris, C.L. (2015). Complement, a target for therapy in inflammatory and degenerative diseases. *Nat. Rev. Drug Discov.* 14, 857–877.
10. Siggins, M.K., Davies, K., Fellows, R., Thwaites, R.S., Baillie, J.K., Semple, M.G., Openshaw, P.J.M., Zelek, W.M., Harris, C.L., and Morgan, B.P.; ISARIC4C Investigators (2023). Alternative pathway dysregulation in tissues drives sustained complement activation and predicts outcome across the disease course in COVID-19. *Immunology* 168, 473–492.
11. Pires, B.G., and Calado, R.T. (2023). Hyperinflammation and complement in COVID-19. *Am. J. Hematol.* 98 (Suppl 4), S74–S81.
12. Conway, E.M., and Prydzial, E.L.G. (2022). Complement contributions to COVID-19. *Curr. Opin. Hematol.* 29, 259–265.
13. Holter, J.C., Pischke, S.E., de Boer, E., Lind, A., Jenum, S., Holtén, A.R., Tonby, K., Barratt-Due, A., Sokolova, M., Schjalm, C., et al. (2020). Systemic complement activation is associated with respiratory failure in COVID-19 hospitalized patients. *Proc. Natl. Acad. Sci. USA* 117, 25018–25025.
14. Boussier, J., Yatim, N., Marchal, A., Hadjadj, J., Charbit, B., El Sissy, C., Carlier, N., Pène, F., Mouthon, L., Tharaux, P.L., et al. (2022). Severe COVID-19 is associated with hyperactivation of the alternative complement pathway. *J. Allergy Clin. Immunol.* 149, 550–556.e2.
15. De Nooijer, A.H., Grondman, I., Janssen, N.A.F., Netea, M.G., Willems, L., van de Veerdonk, F.L., Giamarellos-Bourboulis, E.J., Toonen, E.J.M., and Joosten, L.A.B.; RCI-COVID-19 Study Group (2021). Complement activation in the disease course of coronavirus disease 2019 and its effects on clinical outcomes. *J. Infect. Dis.* 223, 214–224.
16. Ma, L., Sahu, S.K., Cano, M., Kuppuswamy, V., Bajwa, J., McPhatter, J., Pine, A., Meizlish, M.L., Goshua, G., Chang, C.H., et al. (2021). Increased complement activation is a distinctive feature of severe SARS-CoV-2 infection. *Sci. Immunol.* 6, eabh2259.
17. Henry, B.M., Szerygyk, I., de Oliveira, M.H.S., Lippi, G., Benoit, J.L., Vikse, J., and Benoit, S.W. (2021). Complement levels at admission as a reflection of coronavirus disease 2019 (COVID-19) severity state. *J. Med. Virol.* 93, 5515–5522.
18. Ceban, F., Kulzhabayeva, D., Rodrigues, N.B., Di Vincenzo, J.D., Gill, H., Subramaniapillai, M., Lui, L.M.W., Cao, B., Mansur, R.B., Ho, R.C., et al. (2023). COVID-19 vaccination for the prevention and treatment of long COVID: a systematic review and meta-analysis. *Brain Behav. Immun.* 111, 211–229.
19. Leatherdale, A., Stukas, S., Lei, V., West, H.E., Campbell, C.J., Hoiland, R.L., Cooper, J., Wellington, C.L., Sekhon, M.S., Prydzial, E.L.G., and Conway, E.M. (2022). Persistently elevated complement alternative pathway biomarkers in COVID-19 correlate with hypoxemia and predict in-hospital mortality. *Med. Microbiol. Immunol.* 211, 37–48.
20. Ali, Y.M., Ferrari, M., Lynch, N.J., Yaseen, S., Dudler, T., Gragerov, S., Demopoulos, G., Heene, J.L., and Schwaible, W.J. (2021). Lectin pathway mediates complement activation by SARS-CoV-2 proteins. *Front. Immunol.* 12, 714511.
21. Gao, T., Zhu, L., Liu, H., Zhang, X., Wang, T., Fu, Y., Li, H., Dong, Q., Hu, Y., Zhang, Z., et al. (2022). Highly pathogenic coronavirus N protein aggravates inflammation by MASP-2-mediated lectin complement pathway overactivation. *Signal Transduct. Targeted Ther.* 7, 318.
22. Stravalaci, M., Pagani, I., Paraboschi, E.M., Pedotti, M., Doni, A., Scavello, F., Mapelli, S.N., Sironi, M., Perucchini, C., Varani, L., et al. (2022). Recognition and inhibition of SARS-CoV-2 by humoral innate immunity pattern recognition molecules. *Nat. Immunol.* 23, 275–286.
23. Chouaki Benmansour, N., Carvelli, J., and Vivier, E. (2021). Complement cascade in severe forms of COVID-19: recent advances in therapy. *Eur. J. Immunol.* 51, 1652–1659.
24. Lamerton, R.E., Marcial-Juarez, E., Faustini, S.E., Perez-Toledo, M., Goodall, M., Jossi, S.E., Newby, M.L., Chapple, I., Dietrich, T., Veenith, T., et al. (2022). SARS-CoV-2 spike- and nucleoprotein-specific antibodies induced after vaccination or infection promote classical complement activation. *Front. Immunol.* 13, 838780.
25. Zelek, W.M., Cole, J., Ponsford, M.J., Harrison, R.A., Schroeder, B.E., Webb, N., Jolles, S., Fegan, C., Morgan, M., Wise, M.P., and Morgan, B.P. (2020). Complement inhibition with the C5 blocker LFG316 in severe COVID-19. *Am. J. Respir. Crit. Care Med.* 202, 1304–1308.
26. Giudice, V., Pagliano, P., Vatrella, A., Masullo, A., Poto, S., Polverino, B.M., Gammaldi, R., Maglio, A., Sellitto, C., Vitale, C., et al. (2020). Combination of ruxolitinib and eculizumab for treatment of severe SARS-CoV-2-related acute respiratory distress syndrome: a controlled study. *Front. Pharmacol.* 11, 857.
27. Laurence, J., Mulvey, J.J., Seshadri, M., Racanelli, A., Harp, J., Schenck, E.J., Zappetti, D., Horn, E.M., and Magro, C.M. (2020). Anti-complement C5 therapy with eculizumab in three cases of critical COVID-19. *Clin. Immunol.* 219, 108555.
28. Annane, D., Heming, N., Grimaldi-Bensouda, L., Frémeaux-Bacchi, V., Vigan, M., Roux, A.L., Marchal, A., Michel, H., Rottman, M., and Moine, P.; Garches COVID 19 Collaborative Group (2020). Eculizumab as an emergency treatment for adult patients with severe COVID-19 in the intensive care unit: a proof-of-concept study. *eClinicalMedicine* 28, 100590.

29. Vlaar, A.P.J., de Bruin, S., Busch, M., Timmermans, S.A.M.E.G., van Zeggeren, I.E., Koning, R., Ter Horst, L., Bulle, E.B., van Baarle, F.E.H.P., van de Poll, M.C.G., et al. (2020). Anti-C5a antibody IFX-1 (vilobelimab) treatment versus best supportive care for patients with severe COVID-19 (PANAMO): an exploratory open-label, phase 2 randomised controlled trial. *Lancet Rheumatol.* *2*, e764–e773.
30. Mastaglio, S., Ruggeri, A., Risitano, A.M., Angelillo, P., Yancopoulou, D., Mastellos, D.C., Huber-Lang, M., Piemontese, S., Assanelli, A., Garlanda, C., et al. (2020). The first case of COVID-19 treated with the complement C3 inhibitor AMY-101. *Clin. Immunol.* *215*, 108450.
31. Ng, N., and Powell, C.A. (2021). Targeting the complement cascade in the pathophysiology of COVID-19 disease. *J. Clin. Med.* *10*, 2188.
32. Son, K., Jamil, R., Chowdhury, A., Mukherjee, M., Venegas, C., Miyasaki, K., Zhang, K., Patel, Z., Salter, B., Yuen, A.C.Y., et al. (2023). Circulating anti-nuclear autoantibodies in COVID-19 survivors predict long COVID symptoms. *Eur. Respir. J.* *61*, 2200970.
33. Muri, J., Cecchinato, V., Cavalli, A., Shanbhag, A.A., Matkovic, M., Biggiogero, M., Maida, P.A., Moritz, J., Toscano, C., Ghovehoud, E., et al. (2023). Autoantibodies against chemokines post-SARS-CoV-2 infection correlate with disease course. *Nat. Immunol.* *24*, 604–611.
34. Cui, L., Fang, Z., De Souza, C.M., Lerbs, T., Guan, Y., Li, I., Charu, V., Chen, S.Y., Weissman, I., and Wernig, G. (2023). Innate immune cell activation causes lung fibrosis in a humanized model of long COVID. *Proc. Natl. Acad. Sci. USA* *120*, e2217199120.
35. Morgan, B.P. (2016). The membrane attack complex as an inflammatory trigger. *Immunobiology* *221*, 747–751.
36. Triantafilou, M., Hughes, T.R., Morgan, B.P., and Triantafilou, K. (2016). Complementing the inflammasome. *Immunology* *147*, 152–164.
37. Dunkelberger, J.R., and Song, W.C. (2010). Complement and its role in innate and adaptive immune responses. *Cell Res.* *20*, 34–50.
38. Proal, A.D., VanElzakker, M.B., Aleman, S., Bach, K., Boribong, B.P., Buggert, M., Cherry, S., Chertow, D.S., Davies, H.E., Dupont, C.L., et al. (2023). SARS-CoV-2 reservoir in post-acute sequelae of COVID-19 (PASC). *Nat. Immunol.* *24*, 1616–1627.
39. Perico, L., Benigni, A., Casiraghi, F., Ng, L.F.P., Renia, L., and Remuzzi, G. (2021). Immunity, endothelial injury and complement-induced coagulopathy in COVID-19. *Nat. Rev. Nephrol.* *17*, 46–64.
40. Van Damme, K.F.A., Hoste, L., Declercq, J., De Leeuw, E., Maes, B., Martens, L., Colman, R., Browaeys, R., Bosteels, C., Verwaerde, S., et al. (2023). A complement atlas identifies interleukin-6-dependent alternative pathway dysregulation as a key druggable feature of COVID-19. *Sci. Transl. Med.* *15*, eadi0252.
41. Bonilla, H., Peluso, M.J., Rodgers, K., Aberg, J.A., Patterson, T.F., Tamburro, R., Baizer, L., Goldman, J.D., Roupael, N., Deitchman, A., et al. (2023). Therapeutic trials for long COVID-19: a call to action from the interventions taskforce of the RECOVER initiative. *Front. Immunol.* *14*, 1129459.
42. Zelek, W.M., Xie, L., Morgan, B.P., and Harris, C.L. (2019). Compendium of current complement therapeutics. *Mol. Immunol.* *114*, 341–352.
43. Murrell, I., Forde, D., Zelek, W., Tyson, L., Chichester, L., Palmer, N., Jones, R., Morgan, B.P., and Moore, C. (2021). Temporal development and neutralising potential of antibodies against SARS-CoV-2 in hospitalised COVID-19 patients: an observational cohort study. *PLoS One* *16*, e0245382.

STAR★METHODS

KEY RESOURCES TABLE

REAGENT or RESOURCE	SOURCE	IDENTIFIER
Antibodies		
Anti-Ba clone D22/3	Hycult Biotech	Cat# HM2379; RRID: N/A
Anti-FB–biotin clone p21/15	Hycult Biotech	Cat# HM2254; RRID: AB_10363968
Anti-iC3b clone 9	In-house	N/A
Anti-C3c–HRP clone bH6	Hycult Biotech	Cat# HM2168; RRID: AB_533007
Anti-TCC clone aE11	Hycult Biotech	Cat# HM2167; RRID: AB_533189
Anti-C8–biotin clone E2	In-house	N/A
Anti-C1q clone 9H10	In-house	N/A
Anti-C1q rabbit polyclonal	In-house	N/A
Anti-C4 rabbit polyclonal	In-house	N/A
Anti-C4–HRP rabbit polyclonal	In-house	N/A
Anti-C3/C3a clone 2898	Hycult Biotech	Cat# HM2075; RRID: AB_533248
Anti-C3d–HRP clone 3	Hycult Biotech	Cat# HM2198; RRID: AB_920411
Anti-FB clone JC1	In-house	N/A
Anti-FB goat polyclonal	CompTech	Cat# A235; RRID: N/A
Anti-C5 clone 10B6	In-house	N/A
Anti-C5–biotin clone 4G2	In-house	N/A
Anti-C9 clone B7	In-house	N/A
Anti-C9–biotin rabbit polyclonal	In-house	N/A
Anti-C1INH rabbit polyclonal	In-house	N/A
Anti-C1INH–HRP rabbit polyclonal	In-house	N/A
Anti-FH clone OX24	In-house	N/A
Anti-FH–HRP clone 36H9	In-house	N/A
Anti-FHR125 clone MBI125	In-house	N/A
Anti-FH clone 35H9	In-house	N/A
Anti-FHR4 clone 4E9	In-house	N/A
Anti-FHR4–HRP clone 150	In-house	N/A
Anti-sCR1 rabbit polyclonal	In-house	N/A
Anti-sCR1–HRP clone MBI35	In-house	N/A
Anti-properdin clone 9.3.4	Hycult Biotech	Cat# HM2283; RRID: N/A
Anti-properdin–HRP clone 2.9	Hycult Biotech	Cat# HM2282; RRID: N/A
Anti-FD rabbit polyclonal	In-house	N/A
Anti-FD–HRP clone D10/4	Hycult Biotech	Cat# HM2258; RRID: AB_10679352
Anti-FI clone 7B5	In-house	N/A
Anti-FI rabbit polyclonal	In-house	N/A
Anti-clusterin clone 2D5	In-house	N/A
Anti-clusterin–HRP clone 4C7	In-house	N/A
Peroxidase AffiniPure donkey anti-mouse IgG (H + L)	Jackson	Cat# 715-035-151-JIR; RRID: AB_2340771
Peroxidase AffiniPure rabbit anti-goat IgG (H + L)	Jackson	Cat# 305-035-045-JIR; RRID: AB_2339403
Peroxidase AffiniPure donkey anti-rabbit IgG (H + L)	Jackson	Cat# 711-035-152-JIR; RRID: AB_10015282
Biological samples		
Human plasma	This study	N/A
Chemicals, peptides, and recombinant proteins		
Ba	CompTech	Cat# A154
iC3b	CompTech	Cat# A115
Properdin	CompTech	Cat# A139
FD	CompTech	Cat# A136
FB	CompTech	Cat# A135
C1INH	Shire Pharma	https://www.cinryze.com
TCC	In-house	N/A
C1q	In-house	N/A

(Continued on next page)

Continued

REAGENT or RESOURCE	SOURCE	IDENTIFIER
C3	In-house	N/A
C5	In-house	N/A
C9	In-house	N/A
FH	In-house	N/A
FHR4	In-house	N/A
FHR125	In-house	N/A
Fl	In-house	N/A
Clusterin	In-house	N/A
Streptavidin–HRP	R&D Systems	Cat# DY998
Critical commercial assays		
Human C1s/C1-INH complex ELISA	Hycult Biotech	Cat# HK399
Human C5a Duoset ELISA	R&D Systems	Cat# DY2037
Human MASP-1/C1-INH complex ELISA	Hycult Biotech	Cat# HK3001
Software and algorithms		
R Studio Desktop version 2023.09.1 + 494	R Studio	https://posit.co/download/rstudio-desktop/
R version 4.3.1	R Core Team	https://www.r-project.org/
data.table version 1.14.8	R Package (CRAN)	https://cran.r-project.org/web/packages/data.table/index.html
tidyverse version 2.0.0	R Package (CRAN)	https://cran.r-project.org/web/packages/tidyverse/index.html
BiocManager version 1.30.22	R Package (CRAN)	https://cran.r-project.org/web/packages/BiocManager/index.html
ROCR version 1.0–11	R Package (CRAN)	https://cran.r-project.org/web/packages/ROCR/index.html
pROC version 1.18.5	R Package (CRAN)	https://cran.r-project.org/web/packages/pROC/index.html
randomForest version 4.7–1.1	R Package (CRAN)	https://cran.r-project.org/web/packages/randomForest/index.html
splitstackshape version 1.4.8	R Package (CRAN)	https://cran.r-project.org/web/packages/splitstackshape/index.html
gdata version 3.0.0	R Package (CRAN)	https://cran.r-project.org/web/packages/gdata/index.html
MASS version 7.3–60	R Package (CRAN)	https://cran.r-project.org/web/packages/MASS/index.html
sjPlot version 2.8.15	R Package (CRAN)	https://cran.r-project.org/web/packages/sjPlot/index.html
sjlabelled version 1.2.0	R Package (CRAN)	https://cran.r-project.org/web/packages/sjlabelled/index.html
sjmisc version 2.8.15	R Package (CRAN)	https://cran.r-project.org/web/packages/sjmisc/index.html
glmnet version 4.1–8	R Package (CRAN)	https://cran.r-project.org/web/packages/glmnet/index.html
gtools version 3.9.5	R Package (CRAN)	https://cran.r-project.org/web/packages/gtools/index.html
ggplot2 version 3.4.4	R Package (CRAN)	https://cran.r-project.org/web/packages/ggplot2/index.html
Hmisc version 5.1–1	R Package (CRAN)	https://cran.r-project.org/web/packages/Hmisc/index.html
corrplot version 0.92	R Package (CRAN)	https://cran.r-project.org/web/packages/corrplot/index.html
lares version 5.2.3.9003	R Package (CRAN)	https://cran.r-project.org/web/packages/lares/index.html
corr version 0.4.4	R Package (CRAN)	https://cran.r-project.org/web/packages/corr/index.html
ggcorrplot version 0.1.4.1	R Package (CRAN)	https://cran.r-project.org/web/packages/ggcorrplot/index.html
FactoMineR version 2.9	R Package (CRAN)	https://cran.r-project.org/web/packages/FactoMineR/index.html
factoextra version 1.0.7	R Package (CRAN)	https://cran.r-project.org/web/packages/factoextra/index.html

RESOURCE AVAILABILITY

Lead contact

Further information and requests for resources and reagents should be directed to and will be fulfilled by the lead contact, B. Paul Morgan (morganbp@cardiff.ac.uk).

Materials availability

This study did not generate new unique reagents.

Data and code availability

All data generated during the course of this study are included in the published article and [supplemental information](#). This paper does not report original code. Any additional information required to reanalyze the data reported in this paper is available from the [lead contact](#) upon request. Raw data files are freely available

for research use via the Cardiff University Research Portal (<https://doi.org/10.17035/d.2024.0305407248>).

EXPERIMENTAL MODEL AND STUDY PARTICIPANT DETAILS

Donors

EDTA plasma samples were collected from age/ethnicity/sex/infection/vaccine-matched healthy convalescent individuals (controls, $n = 79$) and patients with long COVID (cases, $n = 166$). All participants had a clinical history of acute COVID-19 and direct molecular evidence of infection with SARS-CoV-2. Cases were diagnosed according to the National Institute for Health and Care Excellence (NICE) guideline NG188 (<https://www.nice.org.uk/guidance/ng188>). Eligible patients were men and non-pregnant women over the age of 18 years with no alternative explanatory disease and symptoms that persisted for at least 12 weeks after the initial diagnosis of acute COVID-19. The most prevalent symptoms were breathlessness, fatigue, musculoskeletal problems, neuropsychiatric disturbances, and pain (Table 1). One persistent symptom was sufficient for the diagnosis of long COVID. All patients underwent a comprehensive medical evaluation, including chest radiography, electrocardiography, lung function tests (spirometry with gas transfer as indicated and measurement of exhaled nitric oxide), and standard blood tests (autoantibody screens, bone, liver, and kidney function, coagulation screens, full blood count, and markers of nutrition). In 46.8% of controls and 54.8% of cases, the index infection occurred >2 years prior to sample acquisition, which was limited to a time window between February and October 2022. Symptoms were scored individually using a numeric self-rating scale from 0 (no symptom) to 10 (worst possible symptom). Overall general health was scored similarly on an inverse scale from 0 (worst possible) to 10 (best possible). All participants reported age, ethnicity, and sex. Gender and socioeconomic status were not formally assessed in this study. Cohort demographics, symptomatology, and other key features are summarized in Table 1.

Ethics

All participants provided written informed consent in accordance with the principles of the Declaration of Helsinki. Study approval was granted by the Cardiff University School of Medicine Research Ethics Committee (21/55) and by the Health Research Authority and Health and Care Research Wales (20/NW/0240).

Samples

EDTA blood samples were kept on ice immediately after acquisition. Plasma was separated promptly and stored in aliquots at -80°C .

METHOD DETAILS

Immunoassays

Complement components (C1q, C3, C4, FB, C5, and C9), regulators (C1INH, FH, FHR125, FHR4, FI, FD, properdin, sCR1, and clusterin), and activation products (C1s-C1INH, MASP1-C1INH, Ba, iC3b, C5a, and TCC) were quantified using established in-house or commercial ELISAs. For in-house assays, 96-well MaxiSorp plates (Nunc) were coated with the relevant affinity-purified capture antibody overnight at 4°C , blocked with 2% bovine serum albumin (BSA) or 1% non-fat dried milk (NFM) in phosphate-buffered saline containing 0.1% Tween 20 (PBST, Sigma-Aldrich) for 1 h at room temperature (RT), and washed with PBST. Plasma samples and purified protein standards optimally diluted in 0.2% BSA or 0.1% NFM in PBST were then added in duplicate (50 μL /well) and incubated for 1 h at RT. After a further wash with PBST, the relevant detection antibody (biotinylated, unlabeled, or labeled with horseradish peroxidase [HRP] in-house using commercially available kits, Thermo Fisher

Scientific) was added for 1 h at RT. The plates were then washed with PBST, incubated with streptavidin–HRP or a secondary antibody (HRP-labeled anti-IgG or HRP-labeled anti-IgM) as appropriate, washed again with PBST, and developed using O-phenylenediamine dihydrochloride (SIGMAFAST OPD, Sigma-Aldrich) or tetramethylbenzidine (Thermo Fisher Scientific). Reactions were stopped using 5% sulfuric acid, and absorbances were read at 450 nm or 492 nm. Standard curves were fitted using a non-linear regression model. Sample protein concentrations for each analyte were calculated automatically with reference to the corresponding curve using Prism version 9.5.0 (GraphPad). Plasma dilutions for each biomarker were selected to fall within the linear portion of the log standard curve. All assays passed quality control tests, including evaluations of sensitivity, reproducibility, and coefficients of variation within and across assays (each <10%). Individual assay details are provided in [Table S2](#).

Anti-RBD IgG assay

Antibodies against the SARS-CoV-2 spike protein RBD were detected using a direct ELISA.⁴³ In brief, 96-well MaxiSorp plates (Nunc) were coated overnight with recombinant RBD protein (2 µg/mL) at 4°C, blocked with 3% NFM in PBST for 1 h at RT, and washed with PBST. Plasma samples diluted 1 in 50 in 1% NFM in PBST were then added in duplicate and incubated for 2 h at RT. After a further wash with PBST, donkey anti-human IgG F(ab')₂–HRP (Jackson ImmunoResearch) was added for 1 h at RT. The plates were then washed again with PBST and developed using O-phenylenediamine dihydrochloride (SIGMAFAST OPD, Sigma-Aldrich). Absorbance was measured at 492 nm.

Hemolytic assay

Classical pathway hemolytic activity was measured using sheep erythrocytes sensitized with rabbit anti-sheep erythrocyte antiserum (Siemens Amboceptor, Cruinn Diagnostics). Sensitized sheep erythrocytes (EA) were diluted to 2% in HEPES-buffered saline (HBS) comprising 0.01 M HEPES, 0.15 M NaCl, 2 mM CaCl₂, and 1 mM MgCl₂. Plasma samples were diluted sequentially in HBS and then added in duplicate (50 µL/well) with EA (50 µL/well) and HBS (50 µL/well) to a 96-well tissue-culture plate (Nunc). Assays were incubated for 30 min at 37°C. Intact cells were pelleted via centrifugation. Hemolysis was measured by reading absorbance in the supernatant at 540 nm. Percent hemolysis in each experimental well was calculated relative to the negative (0% lysis) and positive control (100% lysis) wells to determine the 50% classical hemolytic dilution (CH₅₀).

QUANTIFICATION AND STATISTICAL ANALYSIS

General statistics

Categorical variables were assessed using the chi-square test, group means were compared using unpaired t tests, and relationships among variables were evaluated using Pearson's correlation. Significance was assigned at $p < 0.05$. All statistical analyses were performed using Prism version 9.5.0 (GraphPad).

Receiver operating characteristic analysis

A series of GLMs using different combinations of protein measurement data with varying complexity were constructed via logistic regression using the base stats package in R, with a binomial model for error distribution and specified link function. Data were randomly split 70/30 into "training" and "test" sets to prevent overfitting and stratified to maintain case/control proportions, and "test" data were reported as AUCs. As the accuracy of each "test" set prediction was equivalent to the true positive rate/false positive rate, the "predictive power" or "reliability" of each model

was defined using the corresponding AUCs. GLMs containing three major confounders (age, sex, and BMI) were compared to GLMs containing the same confounders and each complement protein using the DeLong test to quantify changes in model performance and show the effects of each analyte on the resultant AUCs. Protein levels were adjusted for age and sex and standardized to a mean of 0 and a standard deviation of 1 to maintain equal contributions of each protein to the analyses and prevent bias arising from proteins with wider ranges, and analyses of unadjusted protein levels were used for comparison. A stepAIC model was run to inform the best features to keep in the final model via iterative analysis of AICs. Models with fewer protein measurements were favored to prevent overfitting and promote clinical utility. Sequential combinations of adjusted complement proteins were also included in a separate series of GLMs. The order of inclusion was informed by the ranking of the corresponding AUCs. Complement protein concentration distributions were compared using the Wilcoxon-Mann-Whitney test, and models were compared using ROC curves, with 95% confidence intervals calculated via the default “bootstrap” method across 2,000 replicates for each AUC.

Principal component analysis

The contribution of each measured protein to the overall variance of individual protein levels and samples was assessed via PCA using the *base stats* package in R. Data were scaled and adjusted as described above. Each principal component and the contribution of each protein to the top two principal components, together with the contribution of individual samples to the overall variance, were visualized using *factoextra* with *ggplot2* and *ggpubr* in R.

Data visualization

Data were visualized as cluster plots and histograms using the *ggplot2* package in R. Correlation plots showing the Pearson correlation coefficient (r) for each complement protein quantified in cases versus controls were created using the *base stats* package in R and visualized using the *corrplot* package in R.